4-2009

Using Pedotransfer Functions in Vadose Zone Models for Estimating Groundwater Recharge in Semiarid Regions

Tiejun Wang
University of Nebraska-Lincoln, tiejun.wang@tju.edu.cn

Vitaly A. Zlotnik
University of Nebraska-Lincoln, vzlotnik1@unl.edu

Jirka Šimunek
University of California - Riverside, jiri.simunek@ucr.edu

Marcel G. Schaap
University of Arizona, mschaap@cals.arizona.edu

Using pedotransfer functions in vadose zone models for estimating groundwater recharge in semiarid regions

Tiejun Wang,[1,2] Vitaly A. Zlotnik,[1] Jirka Šimunek,[3] and Marcel G. Schaap[4]

Received 6 February 2008; revised 19 January 2009; accepted 4 February 2009; published 14 April 2009.

[1] Process-based vadose zone models are becoming common tools for evaluating spatial distributions of groundwater recharge (GR), but their applications are restricted by complicated parameterizations, especially because of the need for highly nonlinear and spatially variable soil hydraulic characteristics (SHCs). In an attempt to address the scarcity of field SHC data, pedotransfer functions (PTF) were introduced in earlier attempts to estimate SHCs. However, the accuracy of this method is rarely questioned in spite of significant uncertainties of PTF-estimated SHCs. In this study, we investigated the applicability of coupling vadose zone models and PTFs for evaluating GR in sand and loamy sand soils in a semiarid region and also their sensitivity to lower boundary conditions. First, a data set containing measured SHCs was used in the simulations. A second data set contained correlated SHCs drawn from the covariance matrix of the first data set. The third SHC data set used was derived from a widely used PTF. Although standard deviations for individual parameters were known for this PTF, no covariance matrix was available. Hence, we assumed that the parameters of this PTF were uncorrelated, thereby potentially overestimating the volume of the parameter space. Results were summarized using histograms of GR for various sets of input parameters. Under the unit gradient flow lower boundary condition, the distributions of GR for sand and loamy sand significantly overlap. Values of GR based on mean SHCs (or GR*) generally lie off the mode of the GR distribution. This indicates that the routinely used method of taking GR* as a regional representation may not be viable. More importantly, the computed GR largely depends in a nonlinear fashion on the shape factor n in the van Genuchten model. Under the same meteorological conditions, a coarser soil with a larger n generally produces a higher GR. Therefore, the uncertainty in computed GR is largely determined by the uncertainty in estimated n by PTFs (e.g., mean and standard deviation). Under the constant head lower boundary condition, upward soil moisture flux may exist from the lower boundary. Especially for regions with shallow water tables where upward flux exists, choosing an appropriate lower boundary condition is more important than selecting SHC values for calculating GR. The results show that the distribution of GR is less scattered and GR is more intense if the constant head lower boundary is located at deeper depths.

Citation: Wang, T., V. A. Zlotnik, J. Šimunek, and M. G. Schaap (2009), Using pedotransfer functions in vadose zone models for estimating groundwater recharge in semiarid regions, *Water Resour. Res.*, *45*, W04412, doi:10.1029/2008WR006903.

1. Introduction

[2] Analysis of groundwater sustainability in semiarid areas relies on the knowledge of spatial distributions of groundwater recharge (GR) [*Scanlon et al.*, 2006]. Although various approaches have been developed on the basis of different physical, chemical, mathematical, and isotopic techniques [*Lerner et al.*, 1990; *Hendrickx and Walker*, 1997; *Scanlon et al.*, 2002], estimation of GR still remains one of the most difficult tasks in hydrology [*National Research Council*, 2004], as GR may substantially vary across landscapes because of spatial variations in soil texture, vegetation, climate forcing, and hydrologic boundary conditions. Compared to methods that yield an areal-averaged GR (e.g., catchment water balance method), hydrodynamic process-based vadose zone models are becoming common tools for evaluating GR and its spatial distribution [*Keese et al.*, 2005; *Small*, 2005; *Nolan et al.*, 2007]. However, the use of vadose zone models is usually restricted by complicated parameterizations, especially because of lack of in situ soil hydraulic characteristics (SHCs). Instead of measuring in situ

[1]Department of Geosciences, University of Nebraska at Lincoln, Lincoln, Nebraska, USA.
[2]Now at School of Natural Resources, University of Nebraska at Lincoln, Lincoln, Nebraska, USA.
[3]Department of Environmental Sciences, University of California, Riverside, California, USA.
[4]College of Agriculture and Life Sciences, University of Arizona, Tucson, Arizona, USA.

0043-1397/09/2008WR006903$09.00

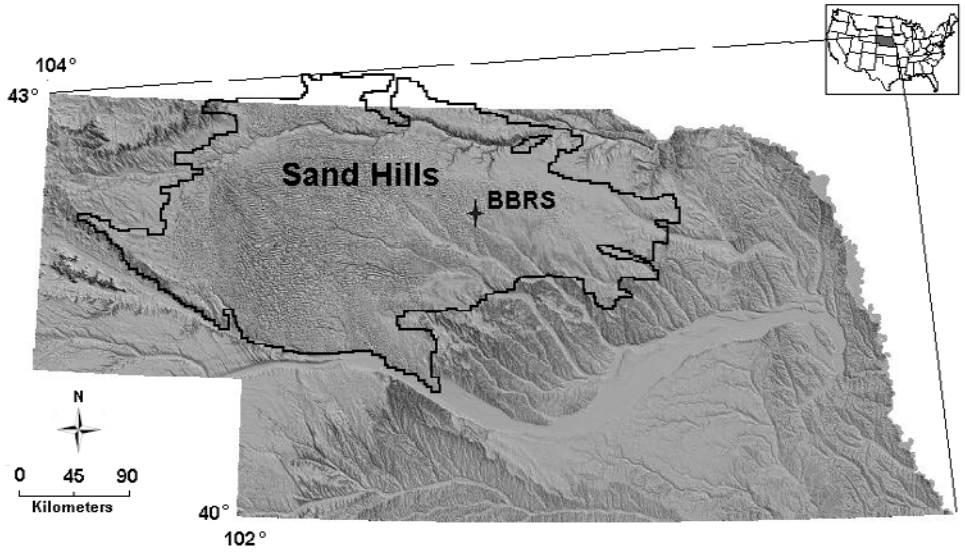

Figure 1. Location of the Barta Brothers Ranch Site (BBRS) in the Nebraska Sand Hills (contoured area indicates the Sand Hills).

SHCs, estimation techniques have been developed such as pedotransfer functions (PTF) [*Wösten et al.*, 2001]. On the basis of regression analysis of existing soil databases, PTFs convert easily measurable soil properties (e.g., soil texture, porosity, and bulk density) to SHCs. With the help of PTFs, vadose zone models have been used for evaluating spatial distributions of GR at large scales [*Nolan et al.*, 2003, 2007; *Keese et al.*, 2005; *Small*, 2005; *Anuraga et al.*, 2006].

[3] Using class-averaged SHCs for different soil textures [*Schaap et al.*, 2001] and a vadose zone model, *Small* [2005] analyzed impacts of soil texture and climatic forcing on GR in the southwestern United States. The study showed that GR can occur from infrequent storms in coarser soils when the ratio of precipitation (P) to potential evapotranspiration (ET_p) exceeds 0.4, but cannot occur in finer soils when $P/ET_p < 0.8$. *Keese et al.* [2005] also used mean SHCs estimated by the Rosetta program [*Schaap et al.*, 2001] to evaluate GR in Texas and assessed impacts of climate, vegetation, and soil texture on GR. The study showed that GR is higher in bare and homogeneous sand and can be reduced by factors of 2–11 for soils whose textures vary with depth. On the basis of a similar method [*Keese et al.*, 2005; *Small*, 2005], *Anuraga et al.* [2006] found that GR in south India is more affected by soil texture than by land use.

[4] Previous studies that coupled vadose zone models and PTFs have shown the significant impact of SHCs on evaluating GR under varying vegetation and climatic conditions. However, the use of mean SHCs for evaluating GR, which is then routinely taken as a regional representation, might be questionable because of significant uncertainties associated with PTF-estimated SHCs [*Schaap and Leij*, 1998; *Schaap et al.*, 2001]. *Nolan et al.* [2007] estimated GR in the eastern United States using both the unit gradient Darcian method with mean SHCs taken from PTFs and a chloride mass balance method. The study showed that the GR estimated by the Darcian method exhibits higher spatial variability because of the uncertainty in estimated SHCs [*Nolan et al.*, 2007]. *Faust et al.* [2006] also pointed out that GR estimated at basin scales depends on the choice of PTFs. It is thus imperative to assess the impact of the uncertainty of PTF-estimated SHCs on GR, especially when using only mean SHCs for GR evaluations [*Keese et al.*, 2005; *Small*, 2005].

[5] In most studies, the unit gradient flow condition is generally assumed at the lower boundary of the vadose zone [*Nolan et al.*, 2003, 2007; *Keese et al.*, 2005; *Small*, 2005]. This boundary implies that water that passes downward across the boundary does not return to the simulated domain. However, such an assumption may not hold in regions of shallow water tables, as studies [*Gillham*, 1984; *Wu et al.*, 1996; *Batelaan et al.*, 2003] have shown significant impacts of water table on GR through processes such as capillary rise or groundwater evapotranspiration.

[6] This study investigates the impact of the uncertainty of PTF-estimated SHCs on computing GR by varying soil texture and lower boundary condition. To be consistent with previous studies, groundwater recharge (GR) is defined here as the amount of water leaving the simulated domain (i.e., lower boundary). A commonly used vadose zone model, Hydrus-1D [*Simunek et al.*, 2005] was chosen because its accuracy has been verified by analytical techniques [*Zlotnik et al.*, 2007]. Soil types of sand and loamy sand were selected. For each soil type, three data sets with the van Genuchten parameters were used. The first data set contained measured SHCs and is referred to as the measured data set. The second data set contained correlated SHCs that were drawn from the covariance matrix of the first data set. The third data set was derived from a widely used PTF [e.g., *Schaap et al.*, 2001]. Although standard deviations for individual parameters were known for this PTF, no covariance matrix was available, and therefore the parameters of the generated SHCs were assumed to be uncorrelated in this study. The hydrometeorological and phenomenological data needed for the simulations were measured at the University of Nebraska's Barta Brothers Ranch Site (BBRS) in the eastern Nebraska Sand Hills.

2. Materials and Methods

2.1. Study Area

[7] This study was performed as a part of the Grassland Destabilization Experiment (GDEX) at the Barta Brothers

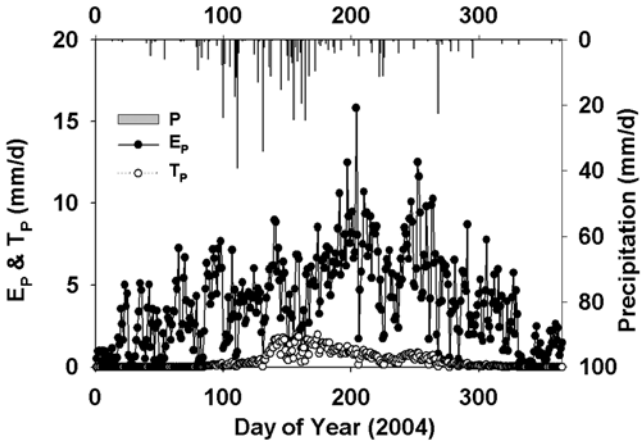

Figure 2. Daily precipitation (P), potential evaporation (E_p), and potential transpiration (T_p) at the GDEX site for the year 2004.

Ranch Site (BBRS) (Figure 1), which investigates the ecological and geomorphic stability of the Nebraska Sand Hills from an interdisciplinary perspective [*Wang et al.*, 2008]. The 58,000 km^2 Nebraska Sand Hills is the largest native grassland-stabilized sand dune field in the Western Hemisphere [*Loope and Swinehart*, 2000]. The high infiltration capacity of sandy soils makes this area an important groundwater recharge source for the Ogallala aquifer. The mean annual temperature at the site is 8.1°C and the mean annual P is 57.6 cm; the mean annual ET_p is 136.0 cm [*Szilagyi et al.*, 2005] and the mean annual humidity index (e.g., P/ET_p) is 0.42. About 90% of the landscape at the BBRS is composed of upland dunes and dry interdunal areas covered by native grasslands, while the remaining 10% consists of wet meadows. Ten circular plots, each 120 m in diameter, were constructed at the site, five of which were equipped with meteorological instruments for evaluating water and energy balances. Surface soils (top 10 cm) are sandy on ridges (average 94.4% sand) and only slightly less sandy in swales (average 91.2% sand). Beneath the 10 cm depth, contents of sand range from 95% to 97% regardless of topographic positions [*Wang et al.*, 2008].

2.2. Flow Model Description

[8] The 1-D Richards equation, describing water flow in saturated and unsaturated porous media, can be formulated as

$$\frac{\partial \theta}{\partial t} = \frac{\partial}{\partial x}\left[K(h)\left(\frac{\partial h}{\partial x}\right) - K(h)\right] - S \tag{1}$$

where θ is volumetric water content; t is time; x is a spatial coordinate; h is water pressure head; S is root water uptake; and K is unsaturated hydraulic conductivity. A commonly used model, Hydrus-1D [*Simunek et al.*, 2005] was utilized for solving equation (1) and computing GR.

[9] The Mualem–van Genuchten model [*van Genuchten*, 1980; *Mualem*, 1976], which analytically describes the relations among θ, h, and K was used:

$$\theta(h) = \theta_r + (\theta_s - \theta_r)/[(1 + |\alpha h|^n)^m], \; h < 0$$
$$\theta(h) = \theta_s, \; h \geq 0 \tag{2}$$

$$K(h) = K_S \times S_e^l \times [1 - (1 - S_e^{1/m})^m]^2 \tag{3}$$

where θ_r is residual soil moisture content; θ_s is saturated soil moisture content; α, n, and l are shape factors: α is inversely related to the air entry pressure, n is a measure of pore size distribution, and lumped parameter l accounts for pore tortuosity and connectivity; $m = 1 - 1/n$; K_S is saturated hydraulic conductivity; and $S_e = (\theta - \theta_r)/(\theta_s - \theta_r)$. The details of the three data sets used in this study are given in Section 3.

[10] The atmospheric upper boundary condition for vadose zone is standard [*Neuman et al.*, 1974]. This boundary condition depends on climatic conditions (i.e., P and potential evaporation E_p) and can switch from a prescribed flux to a prescribed head when limiting pressure heads are exceeded. Surface runoff occurs when P exceeds soil infiltration capacity or soil becomes saturated. Two types of lower boundary conditions were included: unit hydraulic gradient flow condition and constant head condition. For the unit gradient flow boundary, the soil profile depth was 5 m with 201 nodes between the surface and bottom. For the constant head boundary, the soil profile depth was 10 m with 500 nodes between the surface and bottom. Constant heads were set to be 0, 5, and 7 m at the lower boundary, which correspond to zero constant heads at depths of 10, 5, and 3 m below the surface, respectively. To minimize the effect of initial conditions, the simulations were repeated at least 10 times until the soil moisture profiles were equilibrated with climatic forcings [*Keese et al.*, 2005; *Small*, 2005].

[11] The root water uptake was simulated according to the method of *Feddes et al.* [1978], which distributes potential transpiration (T_p) over the root zone on the basis of root density distribution and reduces T_p to actual transpiration on the basis of soil matric potential. The root parameters on pasture were used to determine the Feddes function [*Wesseling*, 1991]. Potential evapotranspiration ET_p was calculated using the Penman-Monteith equation [*Allen et al.*, 1998] and then partitioned into T_p and E_p on the basis of Beer's law [*Ritchie*, 1972]:

$$E_p = ET_p \times e^{-k \times LAI} \tag{4}$$

$$T_p = ET_p - E_p \tag{5}$$

where k is an extinction coefficient set to be 0.5 and LAI is leaf area index.

[12] Hydrometeorological data for the year 2004 at the GDEX site were utilized, including P, air temperature, humidity, solar radiation, soil heat flux, and wind speed. P was 49.3 cm/a or 85.6% of the annual mean and ET_p was 160.6 cm/a or 118% of the annual mean. The 2004 humidity index was 0.31, which was lower than the annual mean of 0.42 in this area. The daily P, T_p, and E_p are plotted in Figure 2. Note that low T_p rate is due to the low LAI in the study area. In 3 m deep soil cores analyzed for root biomass, 60–70% of the total root mass occurred in the top 20 cm and 85–90% occurred in the top 50 cm. On the basis of the field observations [*Wang et al.*, 2008], an exponential distribution was fitted to describe the root density distribution, which is consistent with recent literature reviews on the occurrence of root biomass in native grasslands [*Jackson*

Table 1. Pearson Correlation and Covariance Matrices for the Measured Data Set[a]

	Sand						Loamy Sand					
	θ_r	θ_s	$\log_{10}\alpha$	$\log_{10} n$	$\log_{10} K_S$	l	θ_r	θ_s	$\log_{10}\alpha$	$\log_{10} n$	$\log_{10} K_S$	l
θ_r	-	**0.238**	**0.037**	**0.215**	**0.064**	**−0.097**	-	**0.299**	**−0.5106**	**0.761**	**0.533**	**0.030**
θ_s	0.000	-	**0.338**	**−0.0249**	**0.173**	**−0.068**	0.001	-	**0.434**	**−0.1664**	**0.690**	**−0.330**
$\log_{10}\alpha$	0.000	0.005	-	**0.105**	**0.652**	**0.121**	−0.007	0.010	-	**−0.6960**	**0.159**	**−0.123**
$\log_{10} n$	0.002	−0.0003	0.007	-	**0.506**	**0.230**	0.005	−0.002	−0.042	-	**0.175**	**−0.052**
$\log_{10} K_S$	0.002	0.006	0.144	0.081	-	**0.409**	0.013	0.028	0.034	0.018	-	**0.056**
l	−0.005	−0.005	0.056	0.077	0.450	-	0.004	−0.068	−0.134	−0.027	0.103	-

[a]Numbers in bold are the Pearson correlation.

et al., 1996; *Schenk and Jackson*, 2002]. LAI was measured at the site for partitioning ET_p.

3. Data Sets on Soil Hydraulic Characteristics

[13] In this study, three SHC data sets for sand and loamy sand were used. The first data set included measured SHCs and is referred to as the measured data set. In comparison, the other two were generated, with one containing correlated SHCs randomly generated from the measured SHC data set and the other one containing uncorrelated SHCs derived from the database of *Schaap et al.* [2001].

[14] The first data set with measured SHCs was derived from the UNSODA database (see details in work by *Nemes et al.* [2001]) and was previously used by *Schaap and Leij* [2000] and *Schaap and van Genuchten* [2005]. From this database, we derived 51 samples for sand and 19 samples for loamy sand with all samples having a complete set of measured hydraulic parameters (e.g., θ_r, θ_s, α, n, K_S, and l) that are needed to compute GR.

[15] The second data set with correlated SHCs was derived from the measured data set by computing the class average values for θ_r, θ_s, $\log_{10}\alpha$, $\log_{10} n$, $\log_{10} K_S$, and l for sand and loamy sand. A covariance matrix for these parameters was computed for each of the classes (Table 1), which allows us to account for parameter uncertainty as well as correlations among the parameters. Under the assumption that the means and covariance matrix for θ_r, θ_s, $\log_{10}\alpha$, $\log_{10} n$, $\log_{10} K_S$, and l are an adequate statistical description of the parameter distribution for underlying classes of sand and loamy sand, new samples can be drawn with a Monte Carlo procedure to obtain a more complete distribution of parameter combinations. To this end we followed the procedure by *Carsel and Parrish* [1988]. We generated 200 random samples with correlated parameters by multiplying the upper triangular (Choleski) decomposition [*Press et al.*, 1988] of the covariance matrix with vectors containing six N(0,1) randomly distributed numbers. The result was then added to the mean parameters of each class. Means and standard deviations of the generated parameters as well as a visual inspection of all bivariate distributions showed that the generated distributions overlapped the distributions of the measured data set. However, this exercise led to some l with "very" negative values, which can lead to unreasonable $K(\theta)$ relationships that may show increasing conductivities with decreasing water contents [*Durner et al.*, 1999; *Schaap and Leij*, 2000]. Rather than constraining l to yield monotonic $K(\theta)$ relations, we set l to be 0.5 [*Mualem*, 1976] for simplicity because the numerical experiment showed less sensitivity to l in our analyses.

[16] With the above Monte Carlo procedure, the notion of PTF is extended from the traditional class mean parameters to a procedure that also includes parameter uncertainty and correlations with the objective to yield (correlated) distributions of parameters as a prediction [*Carsel and Parrish*, 1988]. To compare with a more traditional approach, class means and standard deviations (σ) published by *Schaap et al.* [2001] (Table 2) were also used in this study. Another reason for picking the database of *Schaap et al.* [2001] is because it has been widely used in various modeling purposes related to vadose zones, such as soil moisture movement and groundwater recharge [*Keese et al.*, 2005; *Small*, 2005; *Miller et al.*, 2007], contaminant transport [*Dann et al.*, 2006], and root water uptake [*Demirkanli et al.*, 2008; *Segal et al.*, 2008], etc. Given the enormous volume of data used, the database of *Schaap et al.* [2001] gives reasonable ranges of variability in SHC parameters. No complete covariance matrix exists for this PTF and for this reason we assume that the parameters are uncorrelated. GR was then calculated on the basis of combinations of (mean $-$ σ), mean, and (mean + σ) for five selected parameters (i.e., θ_s, $\log_{10} K_S$, $\log_{10}\alpha$, $\log_{10} n$, and l), which leads to total $3^5 = 243$ simulations. In order to reduce the number of simulations, $\theta_r = 0.01$ was set as it is unimportant in the GR analysis (see Figures 5a and 6a). Although some of the combinations might not occur in natural conditions, the shape of GR distributions largely depends on mean and σ of the factor n instead of how the SHC data set is formulated as shown in the following section, which does not affect our conclusions.

[17] Table 2 shows mean values and standard deviations of the SHCs for each of the three data sets. Differences are small among those three data sets, especially for the measured and the correlated data sets, which confirms that the distributions of measured and generated parameters are similar. The difference between the uncorrelated data set and the other two data sets is relatively higher because the different data sources they are based on [see *Schaap and Leij*, 1998; *Schaap et al.*, 2001]. The largest differences are found for $\log_{10} K_s$ of sand, and for $\log_{10} n$ and $\log_{10} K_s$ of loamy sand.

[18] It should be noted that the convergence of simulations with higher n values is slow (e.g., $n > 3$). This is because the water content decreases dramatically within a relatively narrow pressure head interval from 0 cm to about -500 cm, and then stays close to the residual water content for lower pressure heads. Consequently, the hydraulic

Table 2. Average Values of Soil Hydraulic Parameters for the Three Data Sets[a]

	Sand							Loamy Sand						
	N	θ_r	θ_s	$\log_{10}\alpha$	$\log_{10} n$	$\log_{10} K_S$	l	N	θ_r	θ_s	$\log_{10}\alpha$	$\log_{10} n$	$\log_{10} K_S$	l
Measured data set	51	0.048	0.379	−1.512	0.464	2.544	−0.149	19	0.061	0.418	−1.493	0.308	2.275	−0.680
		(0.036)	(0.046)	(0.308)	(0.223)	(0.732)	(1.532)		(0.041)	(0.069)	(0.364)	(0.174)	(0.619)	(3.146)
Correlated data set	200	0.056	0.383	−1.517	0.498	2.599	−0.174	200	0.065	0.417	−1.518	0.309	2.405	0.216
		(0.032)	(0.042)	(0.305)	(0.220)	(0.719)	(1.42)		(0.036)	(0.070)	(0.340)	(0.156)	(0.598)	(2.838)
Uncorrelated data set	308	0.053	0.375	−1.450	0.500	2.810	−0.903	201	0.049	0.390	−1.460	0.240	2.020	−0.874
		(0.029)	(0.055)	(0.250)	(0.180)	(0.590)	(0.486)		(0.042)	(0.070)	(0.470)	(0.160)	(0.640)	(0.594)

[a]Standard deviations are given in parenthesis; N is the number of samples in each data set.

capacity has a narrow peak within this pressure head interval and is more or less zero below it. The hydraulic conductivity also decreases dramatically within this interval and is almost zero below it. The combination of these three soil hydraulic functions often causes problems with convergence of the numerical solution for a dry condition where a large change in pressure heads is accompanied by a minimal change in water contents. Certain numerical measures (e.g., reduce the maximum pressure head at the surface) were taken for overcoming this problem.

4. Results and Discussions

[19] These simulations yielded important conclusions on using process-based vadose models for evaluating GR. In the following sections, histograms are systematically used to summarize numerous simulations of GR and to illustrate effects of various parameters and processes on GR.

4.1. Groundwater Recharge Under Unit Gradient Flow Lower Boundary Condition

4.1.1. Impact of Soil Texture on Groundwater Recharge

[20] Under the unit gradient flow condition, the distributions of computed GR and ET_a from the measured SHC data set are plotted in Figure 3. Because of the high infiltration capacity of sand and loamy sand and the use of a spin-up method (e.g., repetition of the climatic data), surface runoff and change in soil moisture storage are usually negligible in the water balance (e.g., <1%), and thus are not analyzed here. Also note that three simulations for both sand and loamy sand are removed from Figure 3 because of low

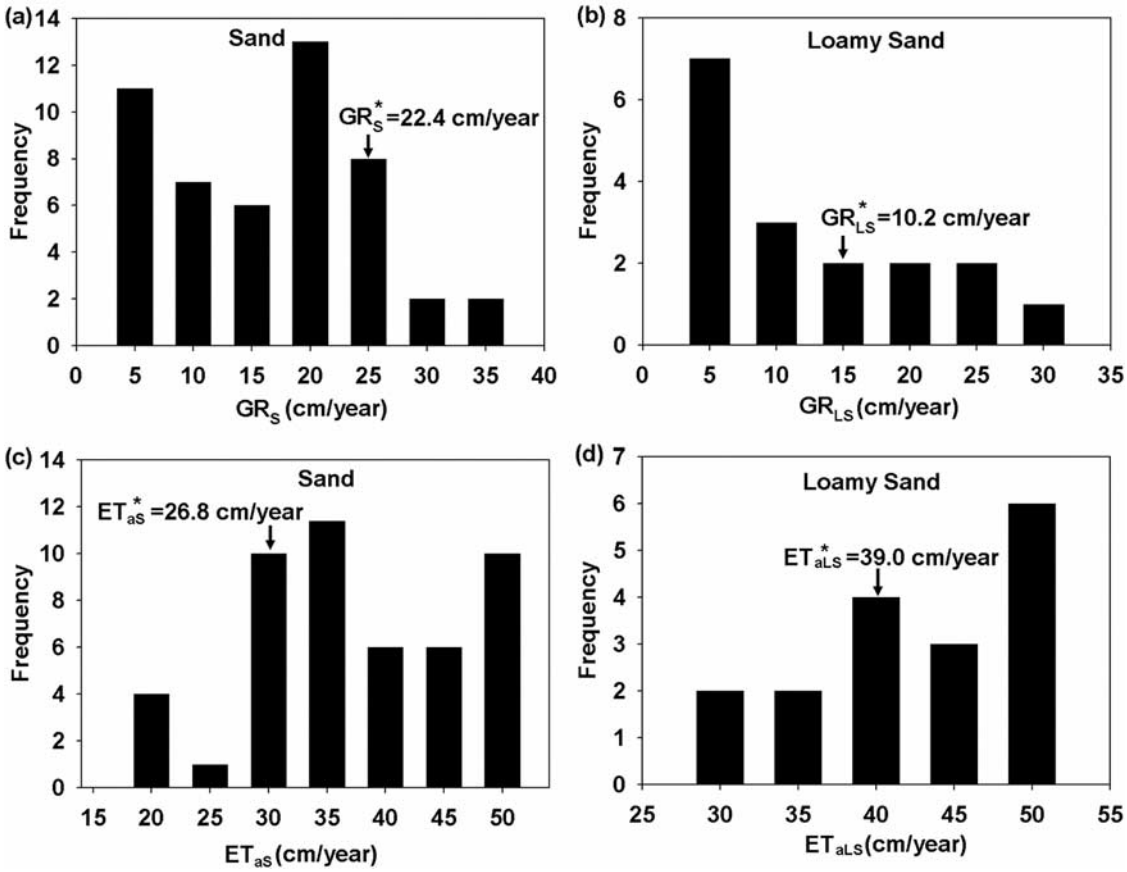

Figure 3. Distributions of groundwater recharge (GR) for (a) sand and (b) loamy sand and actual evapotranspiration (ET_a) for (c) sand and (d) loamy sand based on the measured data set under the unit gradient flow boundary condition. The asterisk represents the results based on mean SHCs. Bin size is 5 cm/a.

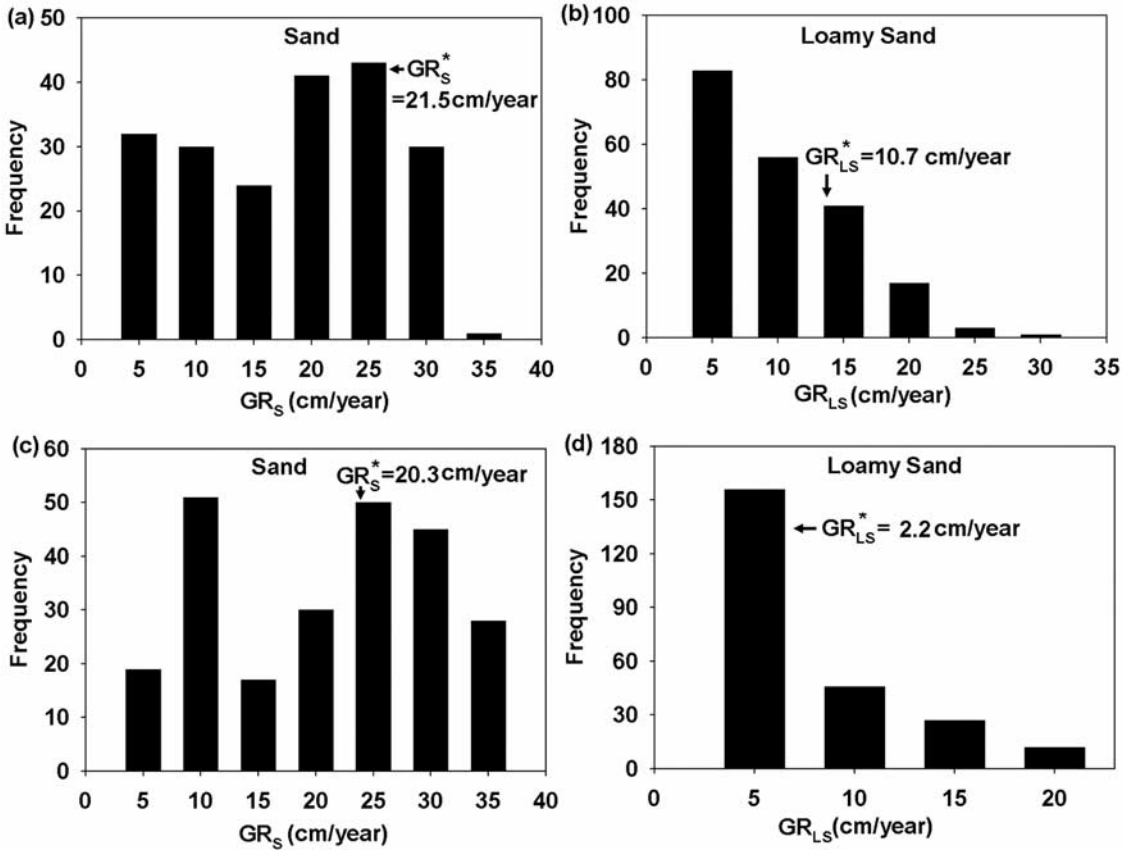

Figure 4. Distributions of groundwater recharge (GR) under the unit gradient flow lower boundary condition: (a) sand and (b) loamy sand from the correlated data set and (c) sand and (d) loamy sand from the uncorrelated data set. The asterisk represents the results based on mean SHCs. Bin size is 5 cm/a.

negative l values, which led to errors of mass balance exceeding 10%, compared to the rest with errors less than <0.5%.

[21] GR for sand (GR_S) ranges from 0.06 to 32.8 cm/a (e.g., <0.01% and 66.5% of the total P, respectively) and ET_a for sand (ET_{aS}) ranges from 16.4 to 49.3 cm/a (e.g., 33.3% and >99.9%, respectively). GR for loamy sand (GR_{LS}) ranges from 0.02 to 25.7 cm/a (e.g., <0.01% and 52.1%, respectively) and ET_a for loamy sand (ET_{aLS}) ranges from 28.4 to 48.9 cm/a (e.g., 57.6% and 99.4%, respectively). Although GR in coarser soils (e.g., GR_S) is generally believed to be higher [*Keese et al.*, 2005; *Small*, 2005], Figure 3 clearly shows that the distributions of GR and ET_a overlap for sand and loamy sand. This is because soil texture is solely defined by particle size distribution; other factors (e.g., bulk density, particle arrangement, and organic matter) that determine SHCs also influence GR. Therefore, the practice of using estimated mean SHCs would not be sufficient to embody the whole range of GR, and so caution is needed when computing GR on large scales with estimated mean SHCs [*Keese et al.*, 2005; *Small*, 2005]. Additionally, the distributions of corresponding GR and ET_a look more or less symmetric because of negligible surface runoff and change in soil moisture storage.

[22] GR estimated from mean SHCs (denoted as GR*) is usually used as a regional estimate of GR [e.g., *Nolan et al.*, 2003, 2007; *Keese et al.*, 2005; *Small*, 2005]. On the basis of mean SHCs of the measured data set, GR* and ET_a^*, also from mean SHCs, are given in Figure 3. GR^*_S and GR^*_{LS} are 22.4 and 10.2 cm/a or 45.4% and 20.7% of the total P, respectively. ET^*_{aS} and ET^*_{aLS} are 26.8 and 39.0 cm/a or 54.4% and 79.1% of the total P, respectively. On the basis of the results, GR^*_{LS} is lower than GR^*_S, which is consistent with the results from *Keese et al.* [2005] and *Small* [2005]. However, Figure 3 also reveals that both GR^*_S and GR^*_{LS} lie off from the peaks on the histograms (Figure 3), which correspond to the highest frequency of the computed GR. Particularly, GR^*_S occurs in neither of the two peaks (Figure 3a). To further illustrate this, the averages of GR were calculated from the distributions in Figure 3, with averages of 13.8 cm/a for sand and 9.5 cm/a for loamy sand. It is obvious that the difference between the average GR and GR^*_S for sand is larger than that for loamy sand, and GR^*_S is thus less representative in a relative sense. This is due to the larger standard deviation of the parameter n for sand (Table 2), the reason of which will be explained in the following section. In general, mean SHCs possess higher occurrence probabilities; however, from Figure 3, using mean SHCs does not imply that GR* also corresponds to the mode of the GR distribution, which is due to the nonlinear relationships between GR and SHCs.

[23] Results from the PTF-generated correlated and uncorrelated SHC data sets are plotted in Figure 4. Because the distributions of corresponding GR and ET_a look also symmetric for the correlated and uncorrelated SHC data

sets, the results of ET_a are thus not presented. For the correlated data set, GR_S ranges from 0.3 to 30.7 cm/a (e.g., <0.01% and 62.3% of the total P, respectively), and GR_{LS} ranges from 0.2 to 27.5 cm/a (e.g., <0.01% and 55.8%, respectively). For the uncorrelated data set, GR_S ranges from 2.5 to 33.4 cm/a (e.g., 5.1% and 67.7%, respectively), and GR_{LS} ranges from 0.07 to 19.1 cm/a (e.g., 0.14% and 38.7%, respectively). In general, results from the measured and generated data sets exhibit similar ranges and patterns of GR. GR^*_S and GR^*_{LS} are 21.5 and 10.7 cm/a (e.g., 43.6% and 21.7% of the total P, respectively) for the correlated data set and 20.3 and 2.2 cm/a (e.g., 41.2% and 4.5%, respectively) for the uncorrelated data set. In comparison to GR^*_S, GR^*_{LS} from the PTF-generated data sets are very different. Furthermore, both GR^*_S correspond to one of the two peaks in the histograms, whereas GR^*_{LS} of the uncorrelated data set is in the clustered peak and lower than that of the correlated data set that lies off from the peak (Figure 4). The difference between GR^*_{LS} values is due to different soil databases used to generate mean SHCs [*Schaap and Leij*, 1998; *Schaap et al.*, 2001], which is also supported by the conclusion of *Faust et al.* [2006] that estimated GR depends on the choice of PTFs. The simulation results strongly suggest that the method of using PTF-estimated mean SHCs to calculate GR* as a regional representative may be inappropriate, particularly for sand, as estimated GR* depends on the choice of PTFs and original soil databases used to generate mean SHCs as well.

[24] On the basis of a water balance method, the *Nebraska Natural Resources Commission* [1986] estimated that GR accounted for 20 to 30% of annual precipitations in the Sand Hills. *Chen and Hu* [2004] used inverse vadose zone modeling and found that GR ranged from 18% to 30% of annual precipitations at a site similar to the GDEX site in the Sand Hills. Also using a water balance method, *Szilagyi et al.* [2005] estimated that mean GR was about 10% of annual precipitations in the region surrounding the GDEX site. In comparison, given that sand is prevalent at the GDEX site [*Wang et al.*, 2008], all calculated GR^*_S (>40% of the total P) are higher than the above results, even though the humidity index of 0.31 in 2004 was already lower than the annual mean of 0.42 in this area. Interestingly, the GR rate that accounts for 10% of the mean annual precipitation [*Szilagyi et al.*, 2005] is closer to the left peak on the histograms (Figures 3a, 4a, and 4c), whereas GR^*_S is closer to the right one. This also demonstrates that the practice of using mean SHCs to estimate GR is not appropriate, at least in the study area.

4.1.2. Sensitivity Analysis of Groundwater Recharge to Soil Hydraulic Characteristics

[25] Figures 3 and 4 show that the shape of GR distributions varies significantly for different soil textures. In general, the distribution of GR_S exhibits a bimodal pattern, whereas the one of GR_{LS} exhibits a unimodal pattern. The standard deviations of GR from each data set are given in Table 3, which also reveals that the distributions of GR_S are more variable than those of GR_{LS}. To investigate the soil parameters that mostly control the shape of GR distribution, relationships between GR and SHCs (e.g., θ_r, θ_s, α, n, K_S, and l) derived from the measured data set are plotted in Figures 5 and 6. Note that the results from the PTF-generated data sets exhibit a similar pattern in Figures 5 and 6 and therefore are not analyzed here.

[26] Of the van Genuchten parameters, θ_r, θ_s, and K_S have physical meanings, whereas the other three parameters are shape factors: α is inversely related to air entry pressure, n is a measure of pore size distribution, and lumped parameter l accounts for pore tortuosity and connectivity. Strikingly, compared to the shape factors, the distribution of GR is not very sensitive to θ_r, θ_s, and K_S for both sand and loamy sand (Figures 5a, 5b, 5e, 6a, 6b, and 6e), even though those three parameters vary significantly in the measured data set. The results indicate that θ_r, θ_s, and K_S are relatively unimportant for determining GR in semiarid regions, possibly because of low soil moisture content in these regions. This conclusion, however, may not hold in humid regions.

[27] The shape of GR distribution is instead mostly controlled by the factor n (Figures 5d and 6d). Figures 5d and 6d show that GR increases with increasing n values. In general, a coarser soil with larger pore sizes possesses a higher n value, which leads to a higher GR. Physically and mathematically, the factor n controls GR mainly through affecting soil surface evaporation. As n becomes larger, the decrease in hydraulic conductivity with decreasing soil moisture becomes stronger (equation (3)), which prevents upward capillary flow of soil moisture toward the evaporating surface because of low hydraulic conductivity in the surface layer. Soil moisture only a few centimeters below the surface becomes unavailable for evaporation when the surface layer is dry and n is large, which reduces evaporation and therefore increases GR. Additionally, the factor l has a similar effect as the factor n has on soil moisture flux (equation (3)), but to a much lesser degree. On the basis of inverse modeling and Monte Carlo simulations, *Pollacco et al.* [2008] also found that the factor n is crucial for estimating GR under the unit gradient flow condition as well as θ_s. However, we found that θ_s is unimportant for determining GR in our study.

[28] It is important to note that the relationship between GR and n is highly nonlinear (Figures 5d and 6d). When n is approximately less than 4, GR increases rapidly with increasing n, then GR starts to level off when n becomes greater than 4, mostly because of limited precipitations (Figures 5d and 6d). The nonlinearity between GR and n reveals the reason why GR* is different from the GR with the maximum occurrence in the GR distribution (Figure 3), as soil samples with larger n values have more weights for determining GR*. This also causes the tendency of GR* to be higher than the most frequent GR (Figure 3). In conclusion, the spatial variability in n is extremely important for determining an areal-averaged GR and its spatial distribution in semiarid regions. The high uncertainty in n estimated by PTFs, particularly for sand [*Schaap et al.*, 1998], makes the use of PTF-estimated mean SHCs in vadose zone models less reliable.

4.2. Groundwater Recharge Under Constant Head Condition

[29] Most studies that used vadose zone models to estimate GR assumed the unit gradient flow at the lower boundary of the vadose zone [*Nolan et al.*, 2003, 2007; *Keese et al.*, 2005; *Small*, 2005]. However, this boundary condition may not be valid for regions where water tables are shallow because groundwater may return to the atmo-

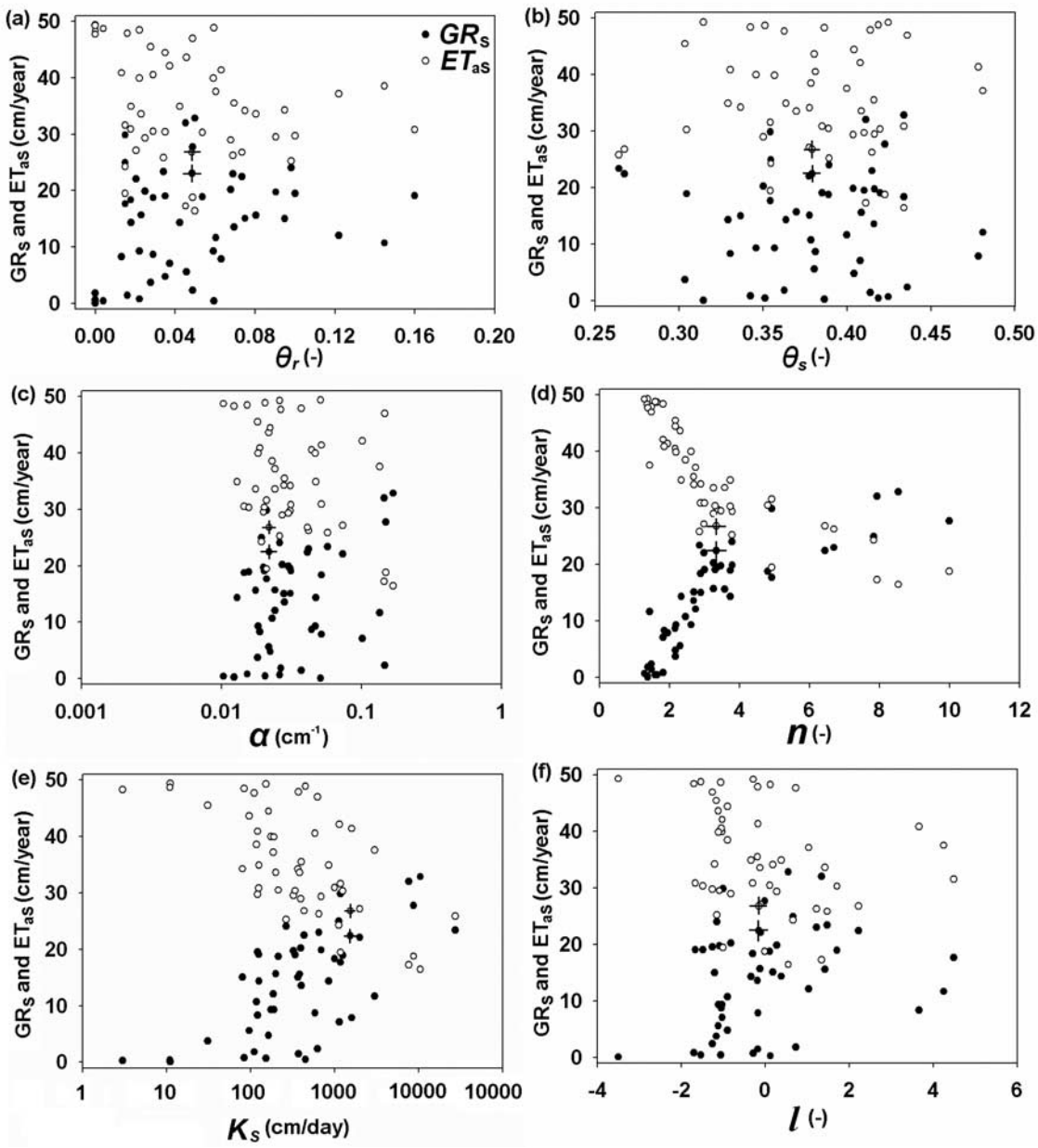

Figure 5. Sensitivity analysis of groundwater recharge (GR_S) and actual evapotranspiration (ET_{aS}) of sand to the van Genuchten parameters: (a) θ_r, (b) θ_s, (c) α, (d) n, (e) K_s, and (f) l. Pluses represent results from mean SHCs.

sphere through either capillary rise or groundwater evapotranspiration [*Gillham*, 1984; *Wu et al.*, 1996; *Batelaan et al.*, 2003]. *Chen and Hu* [2004] used a vadose zone model to study the impact of groundwater on evapotranspiration at a similar site in the NSH. The authors found that the annual evapotranspiration from 1998 to 2000 is 7–21% higher when the groundwater table is included in the model. Therefore, to study the impact of lower boundary conditions on GR, the measured and uncorrelated data sets were used to compute GR. This task was not performed for the correlated data set because previous simulation results showed similar patterns of the GR distributions for the measured and correlated data sets. Constant heads were set to be 0, 5, and 7 m at the lower boundary, which correspond to zero constant heads at depths of 10, 5, and 3 m below the surface, respectively. The simulation results are summarized in Figure 7.

[30] Figure 7 shows that a significant fraction of GR is negative, which implies an upward soil moisture flux from the lower boundary. This obviously differs from the results based on the unit gradient flow lower boundary condition that enforces positive GR values. As explained previously, the factor l has a similar effect on GR as the factor n has. Additional simulations show that if the negative l values in both measured and uncorrelated data sets are replaced by 0.5 as *Mualem* [1976] suggested, the negative GR values would become "less" negative or positive. *Schaap and Leij* [2000] noted the enormously wide range of l values in the literature, and if l becomes more negative, hydraulic conductivity may start increasing with decreasing soil moisture

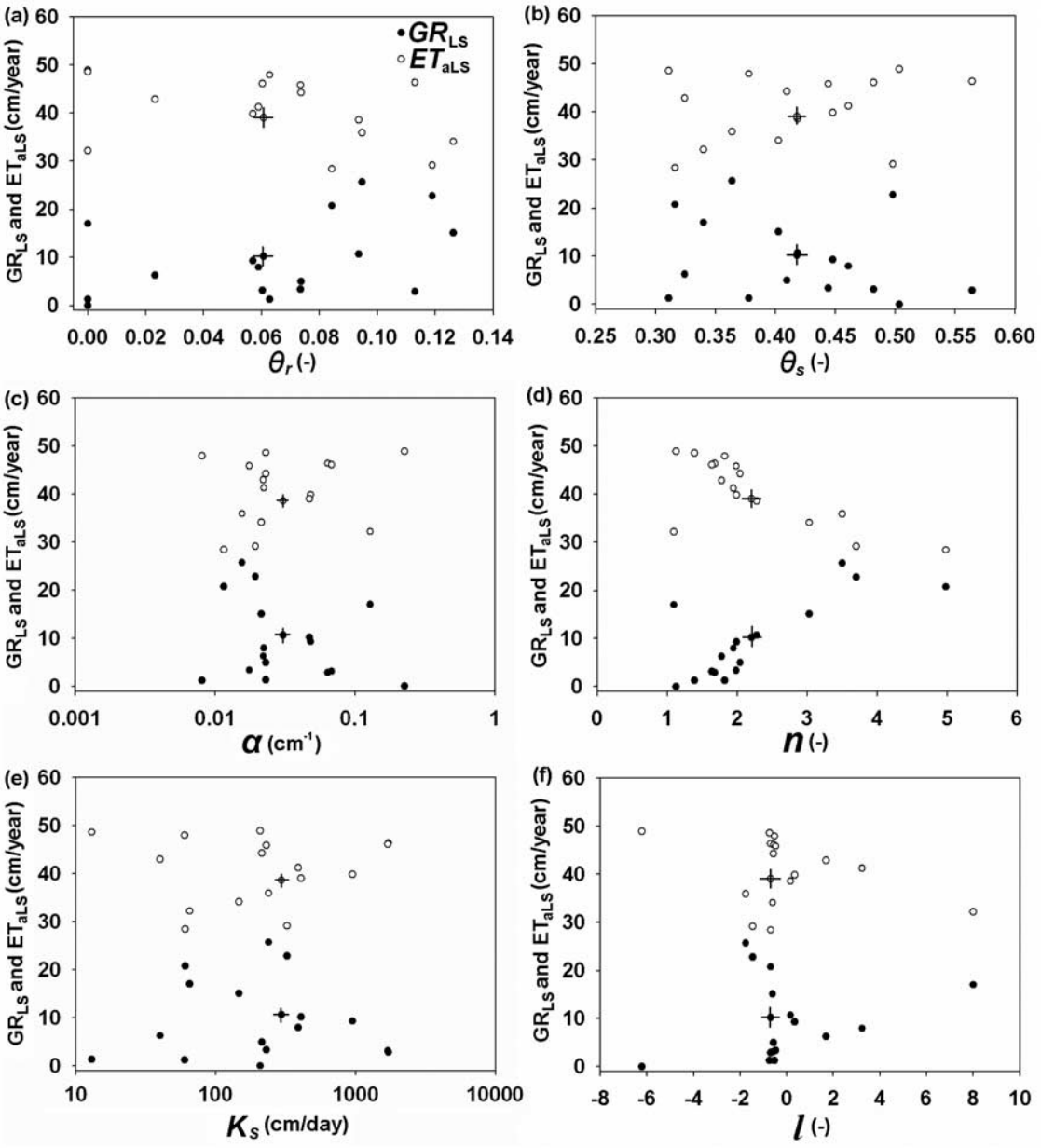

Figure 6. Sensitivity analysis of groundwater recharge (GR_{LS}) and actual evapotranspiration (ET_{aLS}) of loamy sand to the van Genuchten parameters: (a) θ_r, (b) θ_s, (c) α, (d) n, (e) K_s, and (f) l. Pluses represent results from mean SHCs.

content, which is physically unrealistic and can cause unacceptable errors in mass balance as explained previously. If a water table is present, selection of l value may become another important issue. However, because of the wide range of l values [*Schaap and Leij*, 2000], there is still no consensus in the literature on how to select l. Hence, this aspect requires additional study.

[31] Figure 7 also shows that GR with zero constant head at 10 m is higher and its distribution is less scattered than those with zero constant heads at 3 and 5 m depths. Mathematically, a deeper constant head has less influence on the upper atmospheric boundary and simulated domain, allowing more soil moisture to pass downward across the root zone. Table 4 shows GR* under different lower boundary conditions. $GR^*_{\S}$ and GR^*_{LS} generally are more intense under deeper constant head conditions. By varying the lower boundary conditions, the variability in $GR^*_{\S}$ is smaller than the one in GR^*_{LS}. Therefore, the degree of the impact of the lower boundary on the GR distribution depends on soil texture as well. For regions with shallow

Table 3. Standard Deviations of Calculated Groundwater Recharge for Different SHC Data Sets Under the Unit Gradient Flow Boundary Condition

SHC Data Set	Sand (cm/a)	Loamy Sand (cm/a)
Measured	9.15	8.31
Uncorrelated	9.38	4.90
Correlated	8.68	5.28

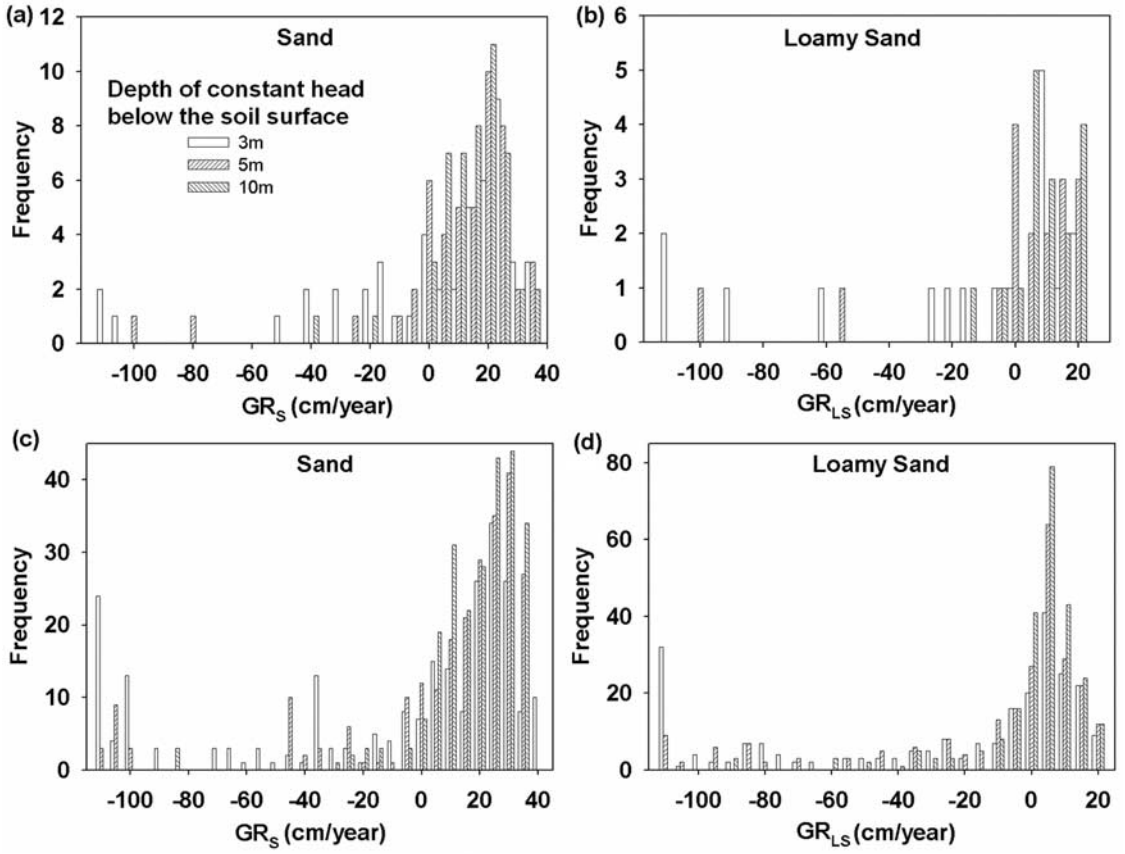

Figure 7. Distributions of groundwater recharge (GR) under the constant head conditions: (a) sand and (b) loamy sand from the measured data set and (c) sand and (d) loamy sand from the uncorrelated data set. Bin size is 5 cm/a.

water depths, as mimicked by the constant head condition in this study, choosing an appropriate lower boundary condition is more important than selecting values of SHCs to estimate GR.

5. Conclusions

[32] In this study, we assessed the applicability of coupling process-based vadose zone models and pedotransfer functions for soil hydraulic characteristics to estimate groundwater recharge in a semiarid region, especially the viability of using PTF-estimated mean SHCs (e.g., soil hydraulic characteristics) to estimate GR [*Nolan et al.*, 2003, 2007; *Keese et al.*, 2005; *Small*, 2005]. Field hydrometeorological and physiological data sets collected in the Nebraska Sand Hills were used to drive the vadose zone model. Three SHC data sets containing the van Genuchten parameters for both sand and loamy sand were used, including a measured, a PTF-generated correlated, and a PTF-generated uncorrelated data set.

[33] Under the unit gradient flow lower boundary condition, the simulation results show that there is a significant overlap in the GR distributions for sand and loamy sand. More importantly, GR* that is estimated from mean SHCs generally lies off from the most frequent range of GR. Therefore, the practice of using mean SHCs to estimate GR is not sufficient, particularly for evaluating GR on large scales [*Nolan et al.*, 2003, 2007; *Keese et al.*, 2005; *Small*, 2005]. It is also found that GR mostly depends on the shape factor n. Coarser soils with larger n values produce higher GR; however, this relationship is highly nonlinear. Because of this nonlinear relationship, GR* tends to be higher than most simulated GR and therefore does not correspond to GR distribution peaks. The spatial variability in n is important for determining an areal-averaged GR and its spatial distribution in semiarid regions. The high uncertainty in estimated n by PTFs, particularly for sand [*Schaap et al.*, 1998], makes the use of PTF-estimated mean SHCs in vadose zone models less reliable. When water tables are present as represented by the constant head conditions in this study, choosing an appropriate lower boundary condition is more important than selecting values of SHCs to estimate GR. Upward soil moisture fluxes may exist from

Table 4. Groundwater Recharge Rate for Different Lower Boundary Conditions[a]

Lower Boundary Condition	Sand (cm/a)		Loamy Sand (cm/a)	
	Measured	Uncorrelated	Measured	Uncorrelated
Unit gradient flow	22.4	20.3	10.2	2.2
Constant head at 3 m	22.6	15.6	7.1	−9.6
Constant head at 5 m	22.6	20.0	10.1	0.3
Constant head at 10 m	22.4	20.6	10.2	2.1

[a]The results are based on mean SHCs of the measured and uncorrelated data sets.

water tables, which is largely controlled by the factor n as well as by the factor l. However, further studies are needed on the criteria for selecting l values. In general, GR is higher and its distribution is less scattered under deeper constant head boundary conditions, the degree of which also depends on soil texture.

[34] **Acknowledgments.** This study was supported by the NSF Biocomplexity program grant DEB 387 0322067 (V. A. Zlotnik and T. Wang), the NSF Hydrologic Sciences Program grants EAR-0609982 (V. A. Zlotnik) and, partially, EAR-0737945 (M. G. Schaap). The authors acknowledge the initial technical review by N. D. Smith (UNL) and valuable suggestions from Editor B. Berkowitz, Associate Editor F. Laio, and three anonymous reviewers that led to significant improvements of this work. The hydrometeorological data sets and soil data sets can be obtained from the corresponding author upon request.

References

Allen, R. G., L. S. Pereira, D. Raes, and M. Smith (1998), Crop evapotranspiration: Guidelines for computing crop water requirements, *Irrig. Drain. Pap. 56*, U. N. Food and Agric. Organ., Rome.

Anuraga, T. S., L. Ruiz, M. S. Mohan Kumar, M. Sekhar, and A. Leijnse (2006), Estimating groundwater recharge using land use and soil data: A case study in South India, *Agric. Water Manage.*, *84*, 65–76, doi:10.1016/j.agwat.2006.01.017.

Batelaan, O., F. De Smedt, and L. Triest (2003), Regional groundwater discharge: Phreatophyte mapping, groundwater modelling and impact analysis of land-use change, *J. Hydrol.*, *275*, 86–108, doi:10.1016/S0022-1694(03)00018-0.

Carsel, R. F., and R. S. Parrish (1988), Developing joint probability distributions of soil water retention characteristics, *Water Resour. Res.*, *24*(5), 755–769, doi:10.1029/WR024i005p00755.

Chen, X., and Q. Hu (2004), Groundwater influences on soil moisture and surface evaporation, *J. Hydrol.*, *297*, 285–300, doi:10.1016/j.jhydrol.2004.04.019.

Dann, R. L., M. E. Close, R. Lee, and L. Pang (2006), Impact of data quality and model complexity on prediction of pesticide leaching, *J. Environ. Qual.*, *35*, 628–640, doi:10.2134/jeq2005.0257.

Demirkanli, D. I., F. J. Molz, D. I. Kaplan, and R. A. Fjeld (2008), A fully transient model for long-term plutonium transport in the Savannah river site vadose zone: Root water uptake, *Vadose Zone J.*, *7*, 1099–1109, doi:10.2136/vzj2007.0134.

Durner, W., B. Schultze, and T. Zurmül (1999), State-of-the-art in inverse modeling of inflow/outflow experiments, in *Characterization and Measurements of the Hydraulic Properties of Unsaturated Porous Media*, edited by M. T. van Genuchten, F. J. Leij, and L. Wu, pp. 661–681, Univ. of Calif., Riverside, Calif.

Faust, A. E., T. P. A. Ferré, M. G. Schaap, and A. C. Hinnell (2006), Can basin-scale recharge be estimated reasonably with water-balance models?, *Vadose Zone J.*, *5*, 850–855, doi:10.2136/vzj2005.0109.

Feddes, R. A., P. J. Kowalik, and S. P. Neuman (1978), *Simulation of Field Water Use and Crop Yield*, John Wiley, New York.

Gillham, R. W. (1984), The capillary fringe and its effect on water-table response, *J. Hydrol.*, *67*, 307–324, doi:10.1016/0022-1694(84)90248-8.

Hendrickx, J., and G. Walker (1997), Recharge from precipitation, in *Recharge of Phreatic Aquifers in (Semi-) Arid Areas*, edited by I. Simmers, pp. 19–98, A. A. Balkema, Rotterdam, Netherlands.

Jackson, R. B., J. Canadell, J. R. Ehleringer, H. A. Mooney, O. E. Sala, and E. D. Schulze (1996), A global analysis of root distributions for terrestrial biomes, *Oecologia*, *108*, 389–411, doi:10.1007/BF00333714.

Keese, K. E., B. R. Scanlon, and R. C. Reedy (2005), Assessing controls on diffuse groundwater recharge using unsaturated flow modeling, *Water Resour. Res.*, *41*, W06010, doi:10.1029/2004WR003841.

Lerner, D. N., A. S. Issar, and I. Simmers (1990), Groundwater recharge, a guide to understanding and estimating natural recharge, *Rep. 8*, 345 pp., Int. Assoc. of Hydrogeol., Kenilworth, U. K.

Loope, D., and J. Swinehart (2000), Thinking like a dune field: Geologic history in the Nebraska Sand Hills, *Great Plains Res.*, *10*, 5–35.

Miller, G. R., D. D. Baldocchi, B. E. Law, and T. Meyers (2007), An analysis of soil moisture dynamics using multi-year data from a network of micrometeorological observation sites, *Adv. Water Resour.*, *30*, 1065–1081, doi:10.1016/j.advwatres.2006.10.002.

Mualem, Y. (1976), A new model for predicting the hydraulic conductivity of unsaturated porous media, *Water Resour. Res.*, *12*(3), 513–522, doi:10.1029/WR012i003p00513.

National Research Council (2004), *Groundwater Fluxes Across Interfaces*, Natl. Acad. Press, Washington, D. C.

Nebraska Natural Resources Commission (1986), Policy issue study on integrated management of surface water and groundwater, 45 pp., Lincoln, Nebr.

Nemes, A., M. G. Schaap, F. J. Leij, and J. H. M. Wösten (2001), Description of the unsaturated soil hydraulic database UNSODA version 2.0, *J. Hydrol.*, *251*, 151–162, doi:10.1016/S0022-1694(01)00465-6.

Neuman, S. P., R. A. Feddes, and E. Bresler (1974), Finite element simulation of flow in saturated-unsaturated soils considering water uptake by plants, third annual report, *Proj. A10-SWC-77*, Hydraul. Eng. Lab., Technion, Haifa, Israel.

Nolan, B. T., A. L. Baehr, and L. J. Kauffman (2003), Spatial variability of groundwater recharge and its effect on shallow groundwater quality in southern New Jersey, *Vadose Zone J*, *2*, 677–691.

Nolan, B. T., R. W. Healy, P. E. Taber, K. Perkins, K. J. Hitt, and D. M. Wolock (2007), Factors influencing ground-water recharge in the eastern United States, *J. Hydrol.*, *332*, 187–205, doi:10.1016/j.jhydrol.2006.06.029.

Pollacco, J. A. P., J. M. S. Ugalde, R. Angulo-Jaramillo, I. Braud, and B. Saugier (2008), A linking test to reduce the number of hydraulic parameters necessary to simulate groundwater recharge in unsaturated soils, *Adv. Water Resour.*, *31*, 355–369, doi:10.1016/j.advwatres.2007.09.002.

Press, W. H., B. P. Flannery, S. A. Teukolsky, and W. T. Vetterling (1988), *Numerical Recipes in C: The Art of Scientific Computing*, Cambridge Univ. Press, Cambridge, U. K.

Ritchie, J. T. (1972), Model for predicting evaporation from a row crop with incomplete cover, *Water Resour. Res.*, *8*(5), 1204–1213, doi:10.1029/WR008i005p01204.

Scanlon, B. R., R. W. Healy, and P. G. Cook (2002), Choosing appropriate techniques for quantifying groundwater recharge, *Hydrogeol. J.*, *10*, 18–39, doi:10.1007/s10040-001-0176-2.

Scanlon, B. R., K. E. Keese, A. L. Flint, L. E. Flint, C. B. Gaye, W. M. Edmunds, and I. Simmers (2006), Global synthesis of groundwater recharge in semiarid and arid regions, *Hydrol. Processes*, *20*, 3335–3370, doi:10.1002/hyp.6335.

Schaap, M. G., and F. J. Leij (1998), Database-related accuracy and uncertainty of pedotransfer functions, *Soil Sci.*, *163*, 765–779, doi:10.1097/00010694-199810000-00001.

Schaap, M. G., and F. J. Leij (2000), Improved predictions of unsaturated hydraulic conductivity with the Mualem–van Genuchten model, *Soil Sci. Soc. Am. J.*, *64*, 843–851.

Schaap, M. G., and M. T. van Genuchten (2005), A modified Mualem–van Genuchten formulation for improved description of the hydraulic conductivity near Saturation, *Vadose Zone J.*, *5*, 27–34, doi:10.2136/vzj2005.0005.

Schaap, M. G., F. J. Leij, and M. T. van Genuchten (1998), Neural network analysis for hierarchical prediction of soil hydraulic properties, *Soil Sci. Soc. Am. J.*, *62*, 847–855.

Schaap, M. G., F. J. Leij, and M. T. van Genuchten (2001), ROSETTA: A computer program for estimating soil hydraulic parameters with hierarchical pedotransfer functions, *J. Hydrol.*, *251*, 163–176, doi:10.1016/S0022-1694(01)00466-8.

Schenk, H. J., and R. B. Jackson (2002), The global biogeography of roots, *Ecol. Monogr.*, *72*(3), 311–328.

Segal, E., T. Kushnir, Y. Mualem, and U. Shani (2008), Water uptake and hydraulics of the root hair rhizosphere, *Vadose Zone J.*, *7*, 1027–1034, doi:10.2136/vzj2007.0122.

Simunek, J., M. T. van Genuchten, and M. Sejna (2005), The HYDRUS-1D software package for simulating the one-dimensional movement of water, heat, and multiple solutes in variably saturated media, version 3.0, *HYDRUS Software Ser. 1*, 270 pp., Dep. of Environ. Sci., Univ. of Calif., Riverside, Calif.

Small, E. E. (2005), Climatic controls on diffuse groundwater recharge in semiarid environments of the southwestern United States, *Water Resour. Res.*, *41*, W04012, doi:10.1029/2004WR003193.

Szilagyi, J., E. F. Harvey, and J. F. Ayers (2005), Regional estimation of total recharge to ground water in Nebraska, *Ground Water*, *43*, 63–69, doi:10.1111/j.1745-6584.2005.tb02286.x.

van Genuchten, M. T. (1980), A closed-form equation for predicting the hydraulic conductivity of unsaturated soils, *Soil Sci. Soc. Am. J.*, *44*, 892–898.

Wang, T., V. A. Zlotnik, D. Wedin, and K. D. Wally (2008), Spatial trends in saturated hydraulic conductivity of vegetated dunes in the Nebraska Sand Hills: Effects of depth and topography, *J. Hydrol.*, *349*, 88–97, doi:10.1016/j.jhydrol.2007.10.027.

Wesseling, J. G. (1991), Meerjarige simulatie van grondwaterstroming voor verschillende bodemprofielen, grondwatertrappen en gewassen met het model SWATRE, report, DLO-Staring Cent. Wageningen, Netherlands, *Rap., 152*, 63 pp.

Wösten, J. H. M., Y. A. Pachepsky, and W. J. Rawls (2001), Pedotransfer functions: Bridging the gap between available basic soil data and missing soil hydraulic characteristics, *J. Hydrol.*, *251*, 123–150, doi:10.1016/S0022-1694(01)00464-4.

Wu, J., R. Zhang, and J. Yang (1996), Analysis of rainfall-recharge relationships, *J. Hydrol.*, *177*, 143–160, doi:10.1016/0022-1694(95)02935-4.

Zlotnik, V. A., T. Wang, J. L. Nieber, and J. A. Simunek (2007), Verification of numerical solutions of the Richards equation using a traveling wave solution, *Adv. Water Resour.*, *30*, 1973–1980, doi:10.1016/j.advwatres.2007.03.008.

M. G. Schaap, College of Agriculture and Life Sciences, University of Arizona, 524 Shantz Building, Tucson, AZ 85721, USA. (mschaap@cals.arizona.edu)

J. Šimunek, Department of Environmental Sciences, University of California, Geology Building 2320, Riverside, CA 92507, USA. (jiri.simunek@ucr.edu)

T. Wang, School of Natural Resources, University of Nebraska at Lincoln, 521 Hardin Hall, Lincoln, NE 68583, USA. (twang3@unl.edu)

V. A. Zlotnik, Department of Geosciences, University of Nebraska at Lincoln, 214 Bessey Hall, Lincoln, NE 68588, USA. (vzlotnik1@unl.edu)